Nickel foam supported biochar doped Ni-Mo bimetallic oxide for supercapacitor applications

Zhongxin Jin[a, b,1*], Kaijia Hu[a, 1], Feng Lin[a], Siqi Liu[a], Ruining Gu[a], Wei Zhang[a], Siyu Liu[a], Caiying Li[a], Hongyang Liao[a], Xinping Cai[a], Haijun Pang[b], Chunjing Zhang[c, d, *], Huiyuan Ma[b, *]

[a]Key Laboratory of Oilfield Applied Chemistry and Technology, College of Chemical Engineering, Daqing Normal University, Daqing 163712, P. R. China.

[b]School of Materials Science and Chemical Engineering, Harbin University of Science and Technology, Harbin 150040, P. R. China.

[c]College of Pharmaceutical Sciences, Heilongjiang University of Chinese Medicine, Harbin 150040, P. R. China.

[d]Key Laboratory of Optic-electric Sensing and Analytical Chemistry for Life Science, MOE.

*Corresponding author. Zhongxin Jin, *E-mail: jzx1128@126.com,* Tel./fax: +86-0451-86392716.

*Corresponding author. Chunjing Zhang, *E-mail: zhangcj922@163.com,* Tel./fax: +86-0451-86392716.

*Corresponding author. Huiyuan Ma, *E-mail: mahy017@163.com,* Tel./fax: +86-0451-86392716.

[1]These authors share co-first-authorship.

Content

1. Experimental Section.....3

1.1 Materials.....3

1.2 Synthesis of Polyoxometalate $(NH_4)_4[Ni(II)Mo_6O_{24}H_6]\cdot 5H_2O$ Precursor.....3

1.3 Preparation of Biochar.....4

1.4 Infrared Spectroscopic Analysis of the Polyoxometalates $(NH_4)_4[Ni(II)Mo_6O_{24}H_6]\cdot 5H_2O$ Precursor.....5

1.5 Electrochemical Impedance Spectroscopy.....6

2. Additional Table.....7

1.6 The capacitance retention rate for 10,000 cycles.....10

1.7 The thickness of working electrodes.....10

1.8 The corresponding weight gain of the material.....11

1.9 Comparison with Different Electrode Materials Used for Supercapacitor Research.....11

Reference.....12

1. Experimental Section

1.1 Materials

Ammonium molybdate $(NH_4)_2MoO_4$, analytical grade, Tianjin Chemical Reagent No. 4 Factory. Nickel Sulfate ($NiSO_4$), analytical grade, Tianjin Zhiyuan Chemical Reagent Co, Ltd. Rice husk (RH), regular grade, Anda City, Heilongjiang Province. Hydrochloric acid (HCl), analytical grade, Guangdong Fangxin Biotechnology Co. Ltd. Potassium hydroxide (KOH), analytical grade, Shenyang Huadong Reagent Factory. Acetylene black (C), analytical grade, Tianjin Fuyu Fine Chemical Co, Ltd. Polytetrafluoroethylene (PTFE), 60%, Shanghai Zhanyun Chemical Co, Ltd. Nickel foam (NF), regular grade, Beijing Chemical Plant. Acetone(C_3H_6O), analytical grade, Tianjin Fuyu Fine Chemical Co, Ltd. Anhydrous ethanol(C_2H_5OH), analytical grade, Tianjin Tianli Chemical Reagent Co, Ltd.

1.2 Synthesis of Polyoxometalate $(NH_4)_4[Ni(II)Mo_6O_{24}H_6]\cdot 5H_2O$ Precursor

Weigh 0.7800 g of nickel sulfate hexahydrate and dissolve it in 20 mL of distilled water. Add 5.2000 g of $(NH)_6Mo_7O_{24}\cdot 4H_2O$ to 80 mL of boiling distilled water. Transfer the nickel sulfate solution to a Buchner funnel and slowly add it dropwise to the ammonium molybdate solution. Evaporate the resulting solution over steam. Cool to room temperature to obtain blue Polyoxometalate nickel molybdate crystals, recrystallize twice with water. The yield is 23.8%. As shown in **Equation 1**,

$$6(NH_4)_6Mo_7O_{24}\cdot 4H_2O + 7NiSO_4\cdot 6H_2O = 7(NH_4)_4[NiMo_6O_{24}H_6] + 3H_2SO_4 + 4(NH_4)_2SO_4 + 7H_2O \quad \textbf{Equation 1}$$

1.3 Preparation of Biochar

Take an appropriate amount of rice husk and soak it in a 500 mL beaker. Wash the rice husk repeatedly with distilled water until the water is clear. After thorough cleaning, place the rice husk in an oven at 60°C to dry it for later use

[1]. Place the rice husk into a crucible and then place the crucible on an electric furnace for carbonization. Stir continuously with an iron rod during the carbonization process until the rice husk turns gray, which takes approximately 3 hours. As shown in **Figure S1**, after collecting the rice husk ash, grind the ash. Mix biochar and KOH in 20mL of deionized water and stir for 2 hours, then dry the mixture at 60 ℃ for 24 hours. In a tube furnace, the dehydrated mixture is subjected to a 2-hour heat treatment at a temperature of 500 ℃ to obtain porous biochar as shown in **Figure S2**. Finally, the obtained porous biochar is attached to foam nickel in a certain way to obtain electrode material as shown in **Figure S3**.

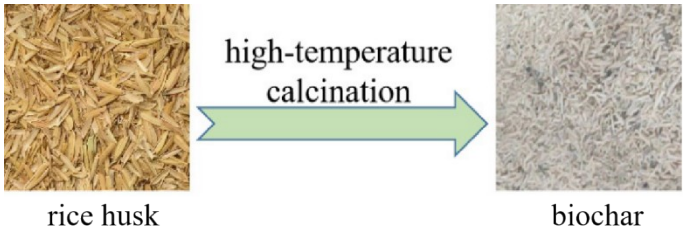

Figure. S1 Preparation of biochar.

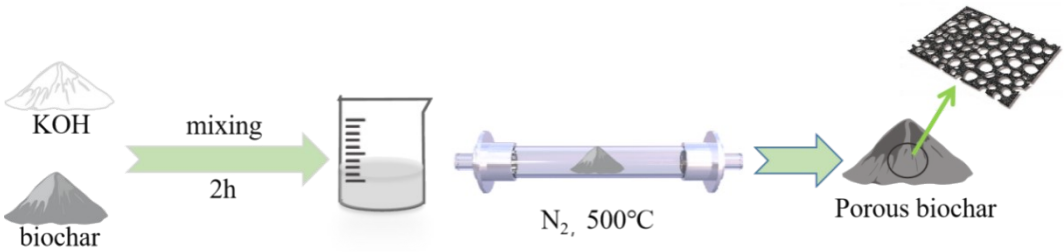

Figure. S2 Preparation of biochar.

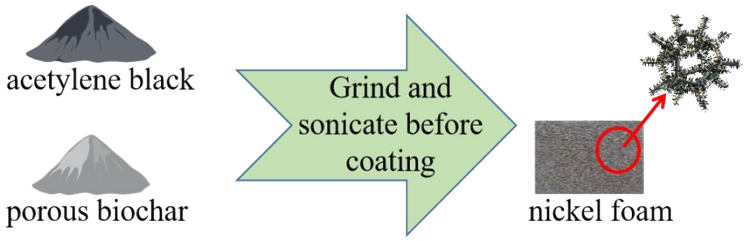

Figure. S3 Preparation of electrode materials.

1.4 Infrared Spectroscopic Analysis of the Polyoxometalates $(NH_4)_4[Ni(II)Mo_6O_{24}H_6]\cdot 5H_2O$ Precursor

The Polyoxometalate $(NH_4)_4[Ni(II)Mo_6O_{24}H_6]\cdot 5H_2O$ was subjected to spectroscopic testing using a Fourier transform infrared (FTIR) spectrometer, covering the wavelength range of 4000 to 400 cm^{-1}. As shown in **Figure S4**, the spectroscopic results indicate that the vibration peak observed at 897 cm^{-1} is attributed to the bending vibration of the Mo-O-Mo bond, while the peak at 934.6 cm^{-1} corresponds to the stretching vibration of the Mo=O bond. Additionally, the peaks observed at 1416 cm^{-1} and 3218 cm^{-1} represent the bending vibration of the H-N-H bond and the stretching vibration of the N-H bond, respectively. The presence of these characteristic peaks confirms the existence of NH_4^+ ions. The vibration peaks at 1664 cm^{-1} and 3345 cm^{-1} correspond to the bending vibration of the H-O-H bond and the stretching vibration of the O-H bond, respectively, indicating the presence of H_2O. This confirms that the prepared precursor is the Polyoxometalates $(NH_4)_4[Ni(II)Mo_6O_{24}H_6]\cdot 5H_2O$[2].

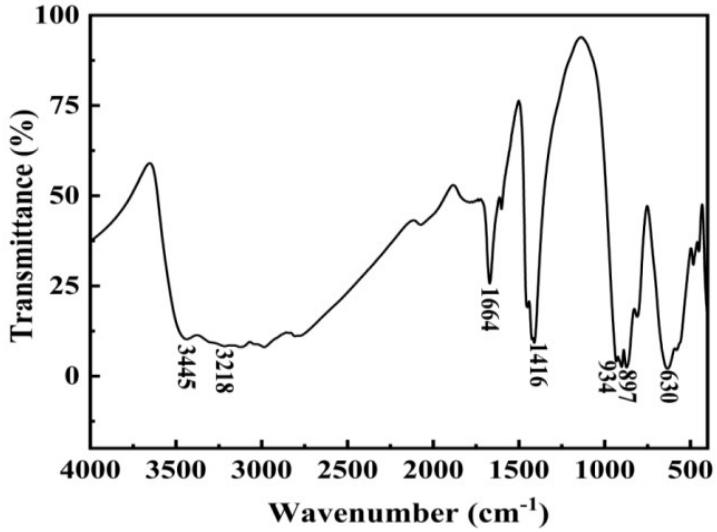

Figure. S4 Infrared Spectrum of $(NH_4)_4[Ni(II)Mo_6O_{24}H_6]\cdot 5H_2O$.

1.5 Electrochemical Impedance Spectroscopy

Figure. S5 shows a Nyquist plot with an equivalent circuit model for C-MoO_3-NiO_2/NF electrode material. The impedance data is fitted using the equivalent circuit model, where Rs (Ω) and Rct (Ω) represent resistance and Warburg impedance, respectively [3]. In the high-frequency region, the charge transfer resistance (Rct) is related to the diameter of the semicircle on the

Nyquist plot, the smaller the diameter of the semicircle, the smaller the charge transfer resistance. And the intercept of the semicircle with the real axis represents the contact resistance Rs, the smaller the intercept in the horizontal axis, the smaller the contact resistance [4-6]. The circuit model parameters are shown in the table below (**Table S4**).

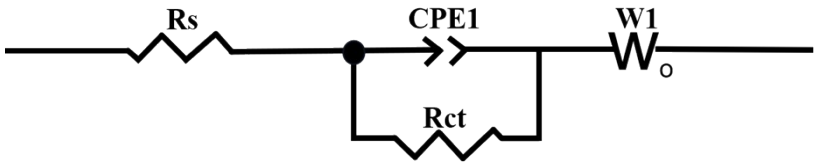

Figure. S5 The equivalent circuit model diagram of C-MoO_3-NiO_2/NF electrode material.

2. Additional Table

As shown in **Table S1**, the charge-discharge performance of C: KOH=1: 1 is the best among the experiments with different C: KOH.

Table S1 Ratio of Biochar and KOH Mixtures.

Serial Number	Biochar	KOH	Times
C: KOH=2: 1	2 g	1 g	268 s
C: KOH=1: 1	2 g	2 g	322 s
C: KOH=1: 2	2 g	4 g	162 s

Table S2 presents the three sets of experiments conducted to investigate the optimal material ratio of the carbon-alkali mixture and polyoxometalates $(NH_4)_4[Ni(II)Mo_6O_{24}H_6]\cdot 5H_2O$, with the increasing mass of polyoxometalates, the constant current charge-discharge time of the samples first increases and then decreases. It can be concluded that the optimal ratio of the carbon-alkali mixture to polyoxometalates is 1:2 (C-MoO_3-NiO_2/NF-2).

Table S2 Ratio of C-MoO_3-NiO_2/NF Mixtures.

Serial Number	Biochar	Polyoxometalates	Times
C-MoO_3-NiO_2/NF-1	0.2 g	0.2 g	39.3 s
C-MoO_3-NiO_2/NF-2	0.2 g	0.4 g	374.4 s

C-MoO_3-NiO_2/NF-3	0.2 g	0.6 g	133.9 s

Table S3 presents comparative experiments of C: KOH=1: 1, C-MoO_3-NiO_2/NF-2 and C: $NiMo_6$ to explore the optimal composite material. The C-MoO_3-NiO_2/NF-2 electrode material presents the best charge-discharge performance.

Table S3 Comparison of composite material.

Serial Number	Biochar	KOH	Polyoxometalates	Times
C: KOH=1: 1	2 g	2 g	—	322 s
C-MoO_3-NiO_2/NF-2	2 g	2 g	0.4 g	374.4s
C: $NiMo_6$	0.2 g	—	0.4 g	151 s

Table S4 Fitting parameters for EIS data for samples of C-MoO_3-NiO_2/NF-2.

Parameters	C-MoO_3-NiO_2/NF-2
Rs	0.43625
Rct	2.724
CPE2-T	0.019968
CPE2-P	0.7257
W1-R	45.18
W1-T	1.776
W1-P	0.59596

Table S5 Comparison of the Resistance of Electrode Materials Treated with Different Carbon-Alkali Ratios

Parameter	C: KOH=1: 1	C: KOH=1: 2	C: KOH=2: 1
Rs	0.59213 Ω	0.7227 Ω	0.71709 Ω
Rct	6.83 Ω	12.36 Ω	9.53 Ω

Table S6 Comparison of the Resistance of Electrode Materials Treated under

Different Conditions

Parameter	C: KOH=1: 1	C-MoO_3-NiO_2/NF	C: $NiMo_6$
Rs	0.59213 Ω	0.48773 Ω	0.55463 Ω
Rct	6.83 Ω	5.42 Ω	6.56 Ω

Table S7 Comparison of the Resistance of Electrode Materials Treated with Different Material Ratios

Parameter	C-MoO_3-NiO_2/NF-1	C-MoO_3-NiO_2/NF-2	C-MoO_3-NiO_2/NF-3
Rs	0.56312 Ω	0.43625 Ω	0.73147 Ω
Rct	37.65 Ω	2.724 Ω	26.59 Ω

1.6 The capacitance retention rate for 10,000 cycles.

The cycling performance of C-MoO_3-NiO_2/NF electrode material for 10000 cycles was conducted to assess cycling stability, and the capacitance retention is 65.4% (**Figure. S6**). Indicating that the C-MoO_3-NiO_2/NF electrode material has good stability and potential application value in in the energy storage field [7].

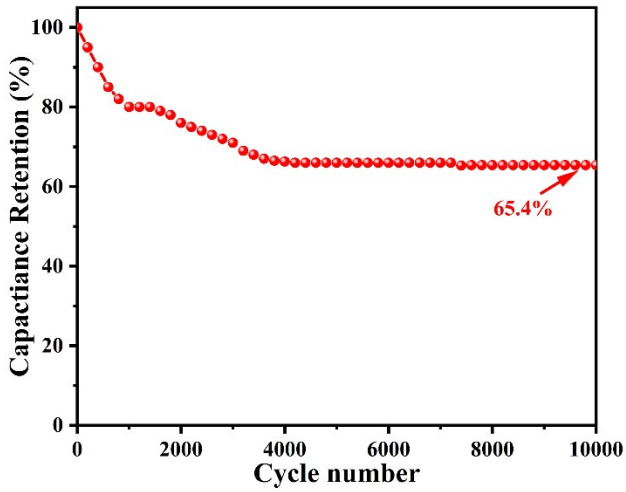

Figure. S6 Cycling stability of C-MoO_3-NiO_2/NF during 10000 cycles at a current density of 1 A/g.

1.7 The thickness of working electrodes.

The thickness of working electrodes was measured by a vernier caliper (**Figure. S7**). The thickness of working electrodes before and after coating is 0.40 mm, 0.50 mm,

respectively.

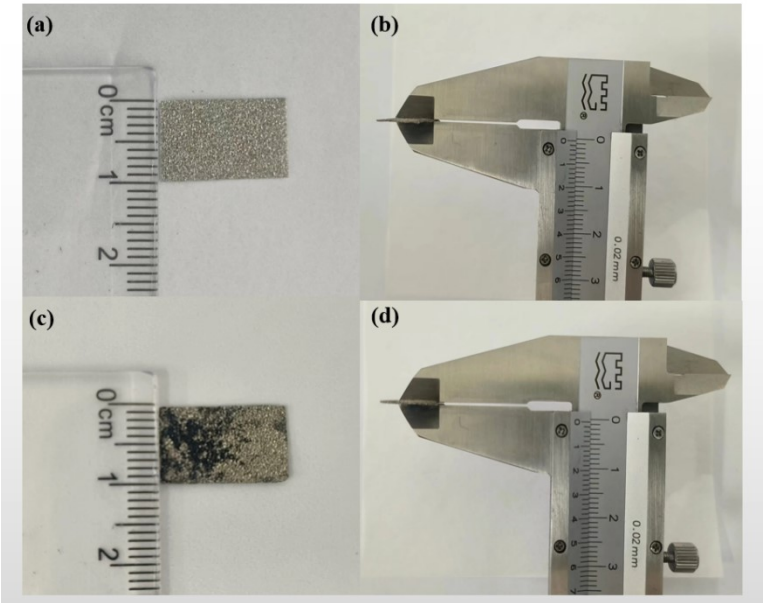

Figure. S7 (a, c) Images of working electrodes before and after coating. (b, d) Graph of working electrodes thickness before and after coating.

1.8 The corresponding weight gain of the material.

m_1 represents the weight of NF before electrode material coating, m_2 represents the weight of NF after electrode material coating. Δm represents the corresponding weight gain of the material.

Table S8. The corresponding weight gain of the material.

Electrode material name	m_1	m_2	Δm
C: KOH=1:1	0.0517 g	0.0534 g	0.0017 g
C: KOH=2:1	0.0571 g	0.0591 g	0.0020 g
C: KOH=1:2	0.0529 g	0.0551 g	0.0022 g
C-MoO_3-NiO_2/NF-1	0.0533 g	0.0551 g	0.0018 g
C-MoO_3-NiO_2/NF-2	0.0519 g	0.0538 g	0.0019 g
C-MoO_3-NiO_2/NF-3	0.0547 g	0.0568 g	0.0021 g
C: $NiMo_6$	0.0528 g	0.0547 g	0.0019 g

1.9 Comparison with Different Electrode Materials Used for

Supercapacitor Research.

Table S9. Comparison with Different electrode materials Used for Supercapacitor Research.

Main components	Specific Capacitance	Capacitance retention rate (%)	Reference
MnO_2/WDB	101 $F \cdot g^{-1}$	85	[8]
Millet straw	144 $F \cdot g^{-1}$	125	[9]
Infested ash tree	123 $F \cdot g^{-1}$	98	[10]
Enteromorpha prolifera	190 $F \cdot g^{-1}$	97.6	[11]
Torreya	136 $F \cdot g^{-1}$	97	[12]
PPy/CNC-COO^--$Cl^-ClO_4^-$)_0.5 SC	125 $F \cdot g^{-1}$	103.3	[13]
PBAC–800	161 $F \cdot g^{-1}$	56.1	[14]
PDA-rGO	120 $F \cdot g^{-1}$	99	[15]
SAC-3	189.4 $F \cdot g^{-1}$	68.6	[16]
Rice husks	180.7 $F \cdot g^{-1}$	75	This work

Reference

[1] Y. H. Bao, H. Xu, P. D. Chen, Y. Q. Zhu, S. S. Zuo, X. Q. Kong, Y. Chen, *New J. Chem.*, 2022, **46**, 14711-14723.

[2] Q. Li, S. X. Li, J. Q. Sha, X. Li, Y. H. Cai, J. H. Yang, J. R. Wang, *ACS Appl. Nano Mater.,* 2021, **4**, 12197–12203.

[3] B. S. Chikkatti, A. M. Sajjan, N. R. Banapurmath, J. K. Bhutto, R. Verma, T. M. Yunus Khan, *Polymers Basel.*, 2023, **15**, 4587.

[4] Y. Q. Zhao, M. Lu, P. Y. Tao, Y. J. Zhang, X. T. Gong, Z. Yang, G. Q. Zhang, H. L. Li, *J. Power Sources*, 2016, **307**, 391- 400.

[5] C. J. Wang, D. P. Wu, H. J. Wang, Z. Y. Gao, F. Xu, K. Jiang, *J. Colloid Interf. Sci.*, 2018, **523**, 133-43.

[6] W. L. Zhang, J. H. Xu, D. X. Hou, J. Yin, D. B. Liu, Y. P. He, H. B. Lin, *J. Colloid Interf. Sci.*, 2018, **530**, 338-44.

[7] H. Guo, H. L. Ren, J. Y. Tian, J. X. Xu, Y. R. Hao, L. P. Peng, Y. S. Liu, W. Yang, *J. Alloys Compd.*, 2024, **1000**, 175107.

[8] C. Wan, Y. Jiao, J. Li, *RSC Adv.*, 2016, **6**, 64811-64817.

[9] Y. Ding, T. Wang, D. Dong, Y. S. Zhang, *Front. Energy Res.*, 2020, **7**, 159.

[10] L. Kouchachvili, N. Maffei, E. Entchev, *J. Porous. Mat.,* 2015, **22**, 979-988.

[11] Y. Gao, R. X. Sun, A. M. Li, G. Z. Ji, *J. Electroanal. Chem.*, 2021, **882**, 114986.

[12] M. Gao, W. K. Wang, Y. M. Zheng, Q. B. Zhao, H. Q. Yu, *Chem. Eng. J.*, 2020, **402**, 126171.

[13] Z. X. Sun, W. Thielemans, *J. Energy Chem.*, 2023, **76**, 165-174.

[14] L. Y. Niu, C. Shen, L. J. Yan, J. H. Zhang, Y. Lin, Y. Y. Gong, C. Li, C. Q. Sun, S. Q. Xu, *J. Colloid Interf. Sci.*, 2019, **547**, 92-101.

[15] S. Dong, Z. Y. Xie, Y. Z. Fang, K. Zhu, Y. Y. Gao, G. L. Wang, J. Yan, K. Cheng, K. Ye, D. X. Cao, *ChemistrySelect.,* 2019, 2711-2715.

[16] F. Ma, S. L. Ding, H. J. Ren, Y. H. Liu, *Rsc. Adv.*, 2019, **9**, 2474.